Journal of Power Sources 196 (2011) 9856–9861

Contents lists available at ScienceDirect

Journal of Power Sources

journal homepage: www.elsevier.com/locate/jpowsour

Radical-induced degradation mechanism of perfluorinated polymer electrolyte membrane

Ryoma Uegaki[a], Yoko Akiyama[a], Sachiko Tojo[b], Yoshihide Honda[b,*], Shigehiro Nishijima[a]

[a] Graduate School of Engineering, Osaka University, Japan
[b] Institute of Scientific and Industrial Research, Osaka University, Japan

ARTICLE INFO

Article history:
Received 24 May 2011
Received in revised form 2 August 2011
Accepted 2 August 2011
Available online 9 August 2011

Keywords:
Nafion
Degradation
PEM
Solution analysis
Radical
γ-Irradiation

ABSTRACT

The degradation mechanism induced by radicals was investigated for Nafion®-117 by solution analysis. Nafion® was exposed independently to three kinds of radicals, $OH^{\bullet}$, $H^{\bullet}$ and $O_2^{\bullet -}$ which were produced separately by γ-irradiation. Based on the eluted elements, the scission site in the membrane was analyzed. The results showed that the scission site was classified into two and these locations were closely relating to oxidative and reductive reactions. The decreasing rate of proton conductivity was more significant under the influence of reductive radicals. The progression of the unzipping reaction of main chain was suggested to be initiated by the production of tertiary carbon radical by reductive radicals such as $H^{\bullet}$ and $O_2^{\bullet -}$ with the aid of $OH^{\bullet}$. The structural degradation such as collapse of cluster and the cluster decomposition as well as the performance degradation was found to be initiated by such reductive radicals.

1. Introduction

To promote fuel cell technology, there are many subjects to be resolved such as dissolution of the platinum [1,2], impurities acting [3,4] and degradation of electrolyte membrane to achieve stable operation with long life. In particular, degradation of polymer electrolyte membrane fuel cell (PEMFC) has been regarded as the major factor [5], and many attempts have been devoted to the elucidation of its degradation mechanism. Degradation process of PEMFC can be classified into two types; mechanical degradation due to repetitive swelling and shrinking associated with variation of temperature and humidity, and chemical and/or electrochemical degradation due to radicals produced via catalytic reaction of platinum. Such chemical degradation is generally thought to play the most important role in the degradation process of PEMFC [5–7]. The radicals such as hydroxy radical ($OH^{\bullet}$), hydrogen radical ($H^{\bullet}$), peroxy radical ($OOH^{\bullet}$) have been thought to be the basic radicals responsible for degradation [8]. Especially a series of formation of these radicals is initiated by $OH^{\bullet}$. There are two kinds of process to produce $OH^{\bullet}$ [5]. One is the direct formation from H_2 and O_2 gasses with platinum catalyst on the electrode and the following reactions to produce $H^{\bullet}$ and $OOH^{\bullet}$ are free from hydrogen peroxide [5,7]. The other is the decomposition of hydrogen peroxide produced by two electron reduction reaction shown bellow [6,9,10]:

$$O_2 + 2H^+ + 2e^- \rightarrow H_2O_2$$

$$H_2O_2 \rightarrow 2OH^{\bullet}$$

$$H_2O_2 + HO^{\bullet} \rightarrow HOO^{\bullet} + H_2O$$

Besides formation mechanism of such radicals, $OOH^{\bullet}$ and $H^{\bullet}$ were detected by ESR measurement in fuel cell testing [6,11]. Superoxide anion ($O_2^{\bullet -}$) was also detected with ESR measurement for the membrane exposed to the Fenton reagent based on Ti (III) [11,12]. Though $O_2^{\bullet -}$ itself might be ignorable in usual fuel cell operation [6], because it was observed only in dry membrane and in low pH condition, it would be valuable to examine the influence of $O_2^{\bullet -}$ on PEMFC. These radicals could be responsible for the polymer decomposition, leading to pinhole formation on the polymer electrolyte surface, depression of proton conductivity, further gas crossover [13]. Fenton reaction is well-known degradation test related to radicals and expressed as follows [14,15]:

$$H_2O_2 + Fe(II) \rightarrow Fe(III) + HO^{\bullet} + HO^-$$

$$Fe(II) + O_2 \leftrightarrow Fe(III) + O_2^{\bullet -}$$

$$HO^{\bullet} + H_2O_2 \rightarrow HOO^{\bullet} + H_2O$$

* Corresponding author.
E-mail address: honda@sanken.osaka-u.ac.jp (Y. Honda).

0378-7753/$ – see front matter © 2011 Elsevier B.V. All rights reserved.
doi:10.1016/j.jpowsour.2011.08.006

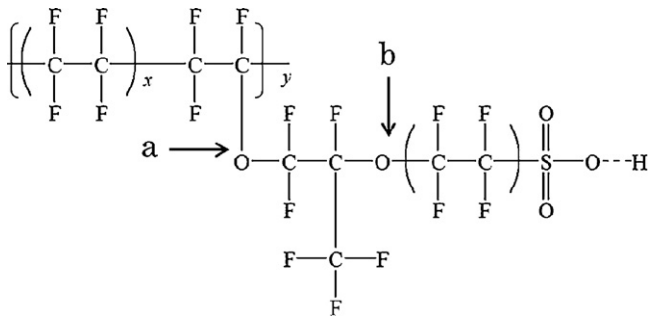

Fig. 1. Chemical structure of Nafion.

However, the radicals produced in Fenton reaction are not exactly the same as the species produced in practical fuel cell operation [16] and multiple reactions including not only radicals but also cations would take place simultaneously, making the analysis of the pathway toward degradation difficult. Even in case of practical fuel cell operation, multiple reactions would take place through the successive reactions such as $OH^{\bullet} + H_2 \rightarrow H^{\bullet} + H_2O$, $H^{\bullet} + O_2 \rightarrow HOO^{\bullet}$. Evaluation of reactivity of each radical species with polymer electrolyte is very important to elucidate the degradation mechanism of polymer electrolyte. The degradation mechanism only due to $OH^{\bullet}$ has been investigated with UV irradiation on hydrogen peroxide solution with PEMFC [17], however the direct observation of degradation process due to other radicals seems not so easy because of the presence of counter ions and/or coexisting radicals.

In our previous studies, the degradation process of Nafion®-117, which is typical perfluorosulfonic acid membrane manufactured by DuPont, was investigated by using Fenton reaction, heat treatment and γ-irradiation [18,19]. In this study, the produced radical species were found to be different among these degradation test. One of the remarkable results obtained in the degradation test due to γ-irradiation was that the amount of the eluted chemical species strongly influenced by the surrounding condition of PEMFC during γ-irradiation, i.e., the membrane was damaged more by the radicals produced in the solvent by γ-ray (indirect effect) rather than those produced directly on the polymer chain (direct effect) [18]. The results suggested that the initiation of degradation due to radicals such as $OH^{\bullet}$ and $H^{\bullet}$, and the following pathway were possibly analyzed by producing such radicals selectively in the solution of PEMFC by γ-irradiation. This method has advantages of without bothering with cationic reactions and multiple reactions, which are induced by the presence of hydrogen peroxide and catalyst. Direct generation of $OH^{\bullet}$ from bound water in the membrane would always take place during γ-irradiation. This amount would not be ignored but can be regarded as smaller compared to the amount of another kinds of radicals produced in solvent, since their concentration is regarded as less than about 20 wt% for Nafion [20]. The objectives of the present research were to examine the reactivity of each radical with PEMFC and to find vulnerable site to the attack of radicals, to elucidate the degradation mechanism of the PEMFC. The radiation damage on PEMFC, especially Nafion, has been reported elsewhere [21–23], however in our study, γ-ray was used only as the tool to produce special kind of radical selectively, and our attention was focused on the following individual radical-induced reactions.

2. Experimental

2.1. Sample preparation

Nafion-117 was used as PEMFC. The chemical structure of Nafion is shown in Fig. 1. The membrane were pretreated with conventional process before irradiation; successive immersion in 3% H_2O_2 solution, ultrapure water, 1 M sulfuric acid solution and ultrapure water for 1 h each. Radicals such as $OH^{\bullet}$, $H^{\bullet}$ and $O_2^{\bullet -}$, were selectively produced by γ-irradiation in solutions, where the radicals were able to be generated quantitatively and uniformly proportional to absorbed dose. Hydroxy radical has been thought to be a principal factor of degradation. It was generated in N_2O saturated water through the reaction shown bellow [24] and the membranes were exposed to $OH^{\bullet}$ during irradiation.

$$e_{aq}^{-} + N_2O + H_2O \rightarrow OH^{\bullet} + N_2 + OH^{-} \quad (1)$$

$O_2^{\bullet -}$ and $H^{\bullet}$ were generated by γ-irradiation in O_2 saturated water and Ar saturated acid (pH 2), respectively [25,26]. Each process is expressed as follows:

$$e_{aq}^{-} + O_2 \rightarrow OH^{\bullet} + O_2^{\bullet -} \quad (2)$$

$$e_{aq}^{-} + H^{+} \rightarrow H^{\bullet} \quad (3)$$

0.5 M *tert*-BuOH was added to these solutions so as to scavenge $OH^{\bullet}$ to generate each radical selectively [27,28]. According to the reactions shown from (1) to (3), the relative production ratio among the generated radical species is able to be evaluated based on the *G* values in water radiolysis, which is the number of product formed by absorbing energy of 100 eV. The *G* values are 2.72 for $OH^{\bullet}$, 2.63 for e_{aq}^{-} and 0.55 for $H^{\bullet}$ [29].

$$OH^{\bullet} : O_2^{\bullet -} : H^{\bullet} = (2.72 + 2.63) : 2.63 : (2.63 + 0.55) \approx 2 : 1 : 1.2$$

Production rate of $OH^{\bullet}$ is almost twice that of other radicals. Nafion (25 mm × 25 mm, 12 pieces) was soaked in 50 mL aqueous solutions prepared according to the procedure mentioned above. The absorbed dose was varied from 0.01 kGy to 1 MGy. The irradiation time was 3 h at low absorbed dose (0.1–100 kGy), while 96 h at high absorbed dose (1 MGy). The absorbed dose was measured by Fricke dosimetry [30].

2.2. Analysis of proton conductivity and eluted species in solutions

The performance of polymer electrolyte after irradiation was evaluated by proton conductivity measured by impedance meter (HIOKI, 3532-80) with four-probe method [31]. The irradiated solutions after taking out the samples were analyzed to evaluate the fragments eluted from polymer electrolyte. Solution analysis is proved to be sensitive and effective in our previous study [18]. The fragment eluted from polymer electrolyte would contain fluorine ion, carbon and sulfur. The eluted chemical components were analyzed by the following methods; fluorine ion and sulfate ion by ion chromatograph (DX-120, Dionex), organic carbon by total organic carbon (TOC) analyzer (IC-V CSH, SHIMADZU) and sulfur by inductively coupled plasma atomic emission spectrometry (ICP-AES) (ICPS-7500, Shimadzu). Proton concentration in the solution was calculated from pH value. The structural change was evaluated by quantifying these eluted species. The solutions in which $O_2^{\bullet -}$ and $H^{\bullet}$ were generated, were evaporated at 85 °C to remove *t*-BuOH, and then the eluted species were dissolved again in 50 mL of ultrapure water.

2.3. Computational analysis

Computational analysis based on molecular orbital theory was also made with MOPAC version 3.9.0. The structure of Nafion was optimized by the PM5 semi-empirical parameters. The chemical properties such as electron density, highest occupied molecular orbital (HOMO), lowest unoccupied molecular orbital (LUMO), formation energy of molecules were evaluated.

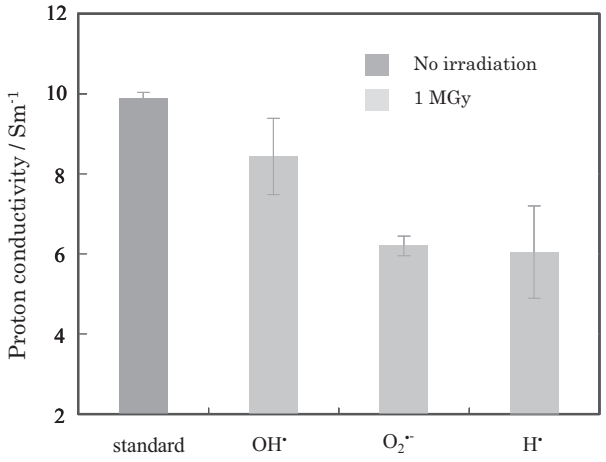

Fig. 2. Proton conductivities of Nafion exposed to several radicals together with non-irradiated Nafion.

3. Results and discussion

3.1. Degradation measurement by proton conductivity

The proton conductivities of Nafion exposed to each radical at 1 MGy are shown in Fig. 2 together with non-irradiated Nafion denoted by "standard". The decrease of proton conductivity was not observed up to absorbed dose of 100 kGy, but was observed at 1 MGy for every samples exposed to different kinds of radicals. In particular, the significant decrease of performance was observed for the samples exposed to $O_2^{\bullet -}$ and H•. It should be noted that the performance of membrane was differently affected by the radical species to which the membrane exposed.

3.2. Scission due to radicals

Presence of eluted fluorine ion in solution is closely related with the degradation of perfluorosulfonic acid membrane prompted by polymer decomposition, and the amount of fluorine ion has been adopted as a measure of degradation level [32,33]. The eluted amounts of chemical species in the solution from Nafion under OH• generated condition are shown in Fig. 3 as a function of absorbed dose. Every species including fluorine ion were increased with increase of absorbed dose. Proton concentration calculated from pH

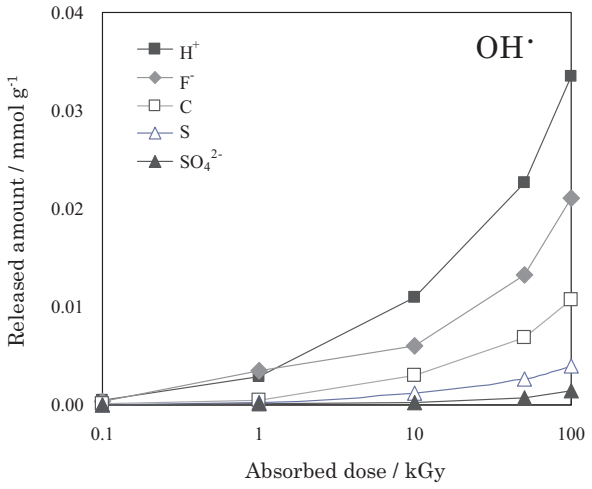

Fig. 3. The amount of dissolved species under exposure to OH• as a function of absorbed dose.

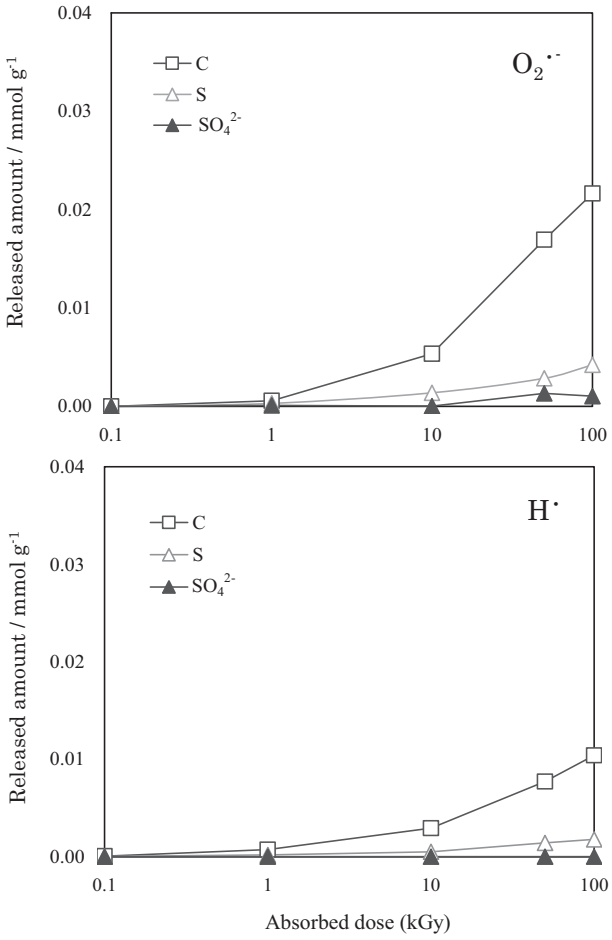

Fig. 4. The amount of dissolved species under exposure to reductive radicals as a function of absorbed dose.

value was also increased, indicating the formation of hydrogen fluoride. The dependencies of the amount of eluted chemical species from Nafion under $O_2^{\bullet -}$ and H• generated conditions on absorbed dose are shown in Fig. 4. Similar behavior was observed for every eluted chemical species except fluorine and hydrogen ions. As the solutions where $O_2^{\bullet -}$ and H• were generated, were evaporated once to remove *t*-BuOH, hydrogen fluoride (boiling point is 19.5 °C) in the solutions was expected to evaporate together, making the quantitative analysis for the concentrations of proton and fluorine ion difficult. Though the amount of generated OH• was almost twice that of other radicals, as shown in Section 2.1, the amount of eluted carbon in OH• generated solution (A) was similar to that in H• generated solution (B) but was almost half of that in $O_2^{\bullet -}$ generated solution (C). On the other hand, the amount of sulfuric ion in the solution (A) was similar to that in the solution (C) but half of that in the solution (B). It is difficult to evaluate reactivity of each radical with polymer chain without knowing reaction pathway. However, if the location of cleavage of polymer chain depends on radical species, the mole ratio of carbon to sulfur (C/S) could be a suitable index to evaluate the scission sites of polymer side chain [18], since sulfur is exclusive to the terminal in side chain. For instance, as Nafion has two ether bonds in the side chain, if the cleavage occurs at the ether bond near main chain ("a" in Fig. 1), C/S would be 5, while the cleavage occurs at the terminal ether bond ("b" in Fig. 1), C/S would be 2. As shown in Table 1, C/S was around 2.6 under OH• generated condition below 100 kGy. This value suggests that the scission at the terminal ether bond in side chain was dominant. On the other hand, the values of C/S under $O_2^{\bullet -}$ and H• generated

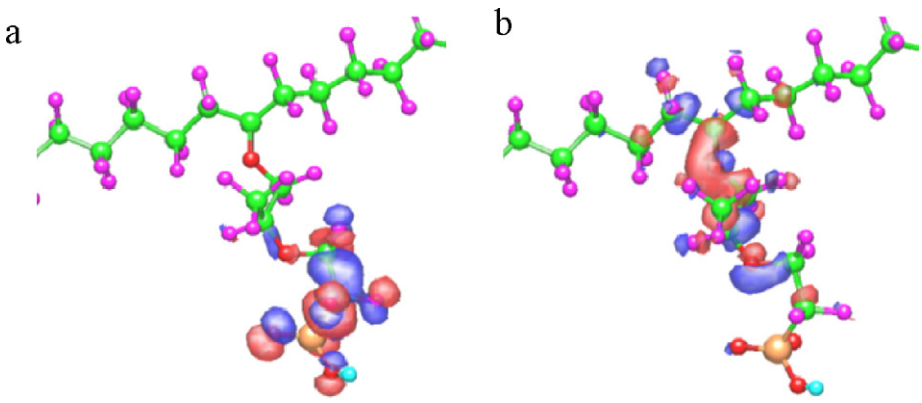

Fig. 5. Optimized geometry of Nafion and their molecular orbitals: (a) HOMO and (b) LUMO.

Table 1
Mole ratio of C to S.

	$OH^{\bullet}$	$O_2^{\bullet-}$	$H^{\bullet}$
10 kGy	2.5	4.1	5.7
50 kGy	2.6	6.0	5.4
100 kGy	2.7	5.1	5.9

condition below 100 kGy were almost more than 5 for each radical species. This value indicates that the whole side chain elution took place for these radicals. Thus which ether bond on side chain is damaged dominantly depends on the radical species to which Nafion is exposed.

Although perfluorosulfonic acid membranes show high chemical stability due to high C–F bond energy, it is widely accepted that the degradation based on unzipping mechanism due to the partially fluorinated end groups [34,13,35]. This degradation process is induced by the attack by $OH^{\bullet}$ to an end group carboxyl acid, followed by hydrogen atom abstraction shown in the following reaction:

$$-CF_2COOH + 2OH^{\bullet} \rightarrow -COOH + CO_2 + 2HF$$

In our results, C/S was around 2 for the attack by $OH^{\bullet}$. If unzipping of main chain was proceeded simultaneously as a dominant degradation process, the mole ratio would become larger. Thus it is reasonable to ignore this process in this context.

3.3. Investigation of radical reactivity by computational analysis

The solution analysis showed that the cleavage at the terminal ether bond in side chain was mainly responsible for the attack by $OH^{\bullet}$, while the cleavage at the ether bond aside of tertiary carbon in main chain was mainly caused by $O_2^{\bullet-}$, $H^{\bullet}$. As $OH^{\bullet}$ is oxidative radical and $O_2^{\bullet-}$, $H^{\bullet}$ have reductive ability [36–38], the radical reactions associated with such radicals were supposed to be related with the oxidation–reduction reaction. On the basis of frontier orbital theory, highest occupied molecular orbital (HOMO) and lowest unoccupied molecular orbital (LUMO) play important roll to initiate electrophilic reaction and nucleophilic reaction. Namely, $OH^{\bullet}$ is expected to be reactive around HOMO, while $O_2^{\bullet-}$ and $H^{\bullet}$ are expected to be reactive around LUMO. The HOMO and the LUMO in Nafion are shown in Fig. 5. Fig. 5 shows that the HOMO and the LUMO are widely distributed around terminal bond in side chain and near main chain, respectively. That is, the reactions associated with oxidative radicals and reductive radicals are expected to take place dominantly around the terminal ether bond in side chain and around the ether bond near main chain, respectively. Furthermore, for the configuration shown in Fig. 5, the leading part of HOMO orbital is relating to the carbon which is located at the right hand side of the terminal ether bond denoted by "b" in Fig. 1, while that of LUMO is in the orbital of the tertiary carbon in main chain.

3.4. Degradation mechanism triggered by radicals

It is well-known that the one of the degradation process of Nafion originates in the termination of main chain with carboxyl group, as shown above. However the possibilities of degradation mechanism attributed to side-chain decomposition are also reported [39,40], and this side-chain decomposition was confirmed by an in situ study of perfluorosulfonic acid membranes with solid-state NMR spectroscopy [41]. Our results also insist the validity of this model.

The reaction mechanism of each kind of radicals in the range below 100 kGy, are able to be explained based on frontier orbital theory, as shown in the previous section. Though the slight mismatch was observed, this could be attributed to the orbital spread over several atoms. The location attacked by $OH^{\bullet}$ is the ether bond, whose energy is weak compared to that of C–C bond [42], and the structure shown in Fig. 6(A) would be formed. The mole ratio of C/S dropped to 1.5 for the solution (A) with dose of 1 MGy (Table 2). This change in C/S is not explained well at this moment, but some possibilities can be shown; the distribution of HOMO was changed from ether bond to C–S bond due to structural change brought by dissociation of sulfonic groups or due to production of new radicals on side chain, or hydrogen bonds were greatly influenced by nonlinear increase of $OH^{\bullet}$, resulting in the form shown in Fig. 6(B). Indeed, the C–S bond is the weakest in the side chain [43] and the cleavage of the C–S bond was indicated from the detection of $-O-CF_2-CF_2^{\bullet}$

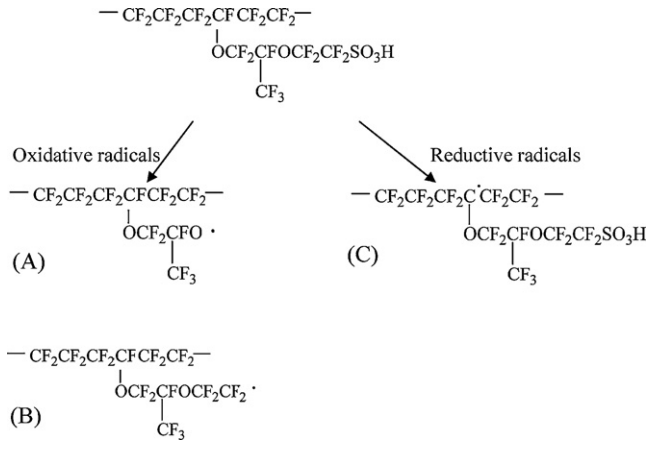

Fig. 6. The degradation mechanism triggered by radicals.

Table 2
Released amount of C and S, and the mole ratio of C to S (1 MGy).

	Produced radicals		
	$OH^{\bullet}$	$O_2^{\bullet-}$	$H^{\bullet}$
Release amount (mmol g^{-1})			
C	0.173	0.454	0.417
S	0.112	0.064	0.059
Mole ratio			
CS^{-1}	1.5	7.1	7.1

radical in the ESR measurements on UV-irradiated membranes in H_2O_2 solutions [12,44]. But once such dissociation happens at side chain, unzipping reactions are thought be proceeded [5], which contradicts the observation. This point have to be studied further.

On the other hand, the cleavage of whole side chain was indicated under the presence of reductive radicals such as $O_2^{\bullet-}$ and $H^{\bullet}$ from the results of solution analysis and molecular orbital calculation. In ESR measurements for UV-induced Fenton treated membranes, the production of tertiary carbon radical in backbone (Fig. 6(C)) is also reported [12,44]. The formation mechanism of tertiary carbon radical can be shown by the reductive radical reaction with C–F bond, followed by the cleavage of ether bond near main chain. Moreover, as shown in Table 2, C/S was 7.1 at 1 MGy for the solutions (B) and (C). This could be explained by the progression of unzipping reaction in main chain, but it seems not to be advanced. This is because the unzipping might be promoted by the residual $OH^{\bullet}$ produced by γ-irradiation in case of higher dose.

3.5. The influence of polymer decomposition on the proton conductivity

The decreasing of proton conductivity due to γ-irradiation was observed at 1 MGy, especially under $O_2^{\bullet-}$ and $H^{\bullet}$ generated condition. Nafion has PTFE backbone of hydrophobic and side chain terminated with hydrophilic sulfonic group, which are phase-separating and then forming cluster structure [45]. The high proton conductivity of such membrane is due to these networked ionic clusters, and the proton conductivity is thought to depend on the number of sulfonic group [13]. As shown in Table 2 and Fig. 2, the desorption of sulfonic group was expected from the high amount of eluted sulfur under $OH^{\bullet}$ generation, however the decreasing rate of proton conductivity was the lowest in spite of the product of $OH^{\bullet}$ being almost twice as shown in Section 2.1. Meanwhile, under $O_2^{\bullet-}$ and $H^{\bullet}$ generation, the depression of proton conductivity was significant and the cleavage of main chain was expected from higher carbon elution. Indeed, estimated from ion exchange capacity of non-irradiated Nafion to be about 0.9 mequiv. g^{-1} [46] and Table 2, the eluted rate of sulfonic groups due to 1 MGy irradiation were about 12% for $OH^{\bullet}$ and 6% for $O_2^{\bullet-}$ and $H^{\bullet}$. As shown in Fig. 2, the decrease in proton conductivity for $OH^{\bullet}$ was about 10%, which is almost as same as the eluted rate of sulfonic group, whereas the significant drop in proton conductivity over 30% was observed for $O_2^{\bullet-}$ and $H^{\bullet}$. These results indicate that the decomposition of cluster accompanied by the scission of main chain causes the serious depression of proton conductivity and that the decrease of sulfonic group is less sensitive to proton conductivity.

4. Conclusion

The radical-induced degradation mechanism of Nafion was investigated with separately produced radicals such as $OH^{\bullet}$, $O_2^{\bullet-}$ and $H^{\bullet}$ by γ-irradiation under special conditions. The side-chain cleavages was observed for all kinds of samples, however the different mechanism of the side-chain decomposition was indicated from the mole ratio of eluted carbon to sulfur; i.e., the location of scission depends on oxidative or reductive ability of radical. The depression of proton conductivity was not observed below 100 kGy, whereas the depression was observed at 1 MGy and was more significant for the samples exposed to $O_2^{\bullet-}$ and $H^{\bullet}$ rather than the sample exposed to $OH^{\bullet}$, though the amount of eluted sulfuric group exposed to $O_2^{\bullet-}$ and $H^{\bullet}$ was not so much compared to that of samples exposed to $OH^{\bullet}$. Furthermore, the progression of unzipping reaction of main chain in addition to the cleavage of side chain, which was confirmed by computational analysis, was observed with solution analysis only for the samples exposed to $O_2^{\bullet-}$ and $H^{\bullet}$. These results indicate that the cleavage of main chain is triggered by the tertiary carbon radical produced by reductive radicals, leading to the structural degradation such as collapse of cluster and the cluster decomposition via performance degradation. Accordingly, it can be said that the prevention of cluster decomposition with main-chain cleavage is primary policy to prevent degradation.

Acknowledgement

We gratefully acknowledge support from NEDO.

References

[1] M. Umeda, T. Maruta, M. Inoue, A. Nakazawa, J. Phys. Chem. C 112 (2008) 18098–18103.
[2] X. Yu, S. Ye, J. Power Sources 172 (2007) 145.
[3] F.N. Cayan, M. Zhi, S.R. Pakalapati, I. Celik, N. Wu, R. Gemmen, J. Power Sources 185 (2008) 595–602.
[4] J. Zhang, H. Wang, D.P. Wilkinson, D. Song, J. Shen, Z.-S. Liu, J. Power Sources 147 (2005) 58–71.
[5] L. Ghassemzadeh, K.-D. Kreuer, J. Maier, K. Müller, J. Phys. Chem. C 114 (2010) 14635–14645.
[6] M. Danilczuk, F.D. Coms, S. Schlick, J. Phys. Chem. B 113 (2009) 8031–8042.
[7] V.O. Mittal, H.R. Kunz, J.M. Fenton, J. Electrochem. Soc. 154 (2007) B652–B656.
[8] L. Gubler, S.M. Dockheer, W.H. Koppenol, J. Electrochem. Soc. 158 (2011) B755–B769.
[9] J. Healy, C. Hayden, T. Xie, K. Olson, R. Waldo, M. Brundage, H. Gasteiger, J. Abbott, Fuel Cells 5 (2005) 302–308.
[10] B. Vogel, H. Dilger, E. Roduner, Macromolecules 43 (2010) 4688–4697.
[11] A. Bosnjakovic, S. Schlick, J. Phys. Chem. B 108 (2004) 4332–4337.
[12] M.K. Kadirov, A. Bosnjakovic, S. Schlick, J. Phys. Chem. B 109 (2005) 7664–7670.
[13] F. Wang, H. Tang, M. Pan, D. Li, Int. J. Hydrogen Energy 33 (2008) 2283–2288.
[14] D.W. Rhoades, M.K. Hassan, S.J. Osborn, R.B. Moore, K.A. Mauritz, J. Power Sources 172 (2007) 72–77.
[15] A. Bosnjakovic, K. Marsil, M.K. Kadirov, S. Schlick, Res. Chem. Intermed. 33 (2007) 677–687.
[16] N.E. Cipollini, ECS Trans. 11 (2007) 1071–1082.
[17] C. Zhou, M.A. Guerra, Z.-M. Qiu, T.A. Zawodzinski Jr., D.A. Schiraldi, Macromolecules 40 (2007) 8695–8707.
[18] Y. Akiyama, H.S. Sodaye, Y. Shibahara, Y. Honda, S. Tagawa, S. Nishijima, J. Power Sources 195 (2010) 5915–5921.
[19] Y. Akiyama, H.S. Sodaye, Y. Shibahara, Y. Honda, S. Tagawa, S. Nishijima, Polym. Degrad. Stab. 95 (2010) 1–5.
[20] Y. Shibahara, Y. Akiyama, Y. Izumi, S. Nishijima, Y. Honda, N. Kimura, S. Tagawa, G. Isoyama, J. Polym. Sci. B 46 (2008) 1–7.
[21] M. Schulze, M. Lorenz, N. Wagner, E. Gülzow, Fresenius J. Anal. Chem. 365 (1999) 106–113.
[22] Y. Iwai, T. Yamanishi, K. Isobe, M. Nishi, T. Yagi, M. Tamada, Fusion Eng. Des. 81 (2006) 815–820.
[23] E.B. Fox, S.D. Greenway, E.A. Clark, Fusion Sci. Technol. 57 (2009) 103–111.
[24] J. Lee, W. Song, S.S. Jang, J.D. Fortner, P.J.J. Alvarez, W.J. Cooper, J.-H. Kim, Environ. Sci. Technol. 44 (2010) 3786–3792.
[25] C.L. Greenstock, G.W. Ruddock, Int. J. Radiat. Phys. Chem. 8 (1976) 367–369.
[26] E. Hayon, M. Simic, J. Am. Chem. Soc. 95 (1973) 2433–2439.
[27] J. Hoigné, H. Bader, Water Res. 17 (1983) 173–183.
[28] M. Carbajo, F.J. Beltrán, F. Medina, O. Gimeno, F.J. Rivas, Appl. Catal. B: Environ. 67 (2006) 177–186.
[29] C.V. Buxton, in: Farhataziz, M.A.J. Rodgers (Eds.), Radiation Chemistry Principle and Practice, CVH Publishers, New York, 1987, pp. 321–349.
[30] G.G. Jayson, B.J. Parsons, A.J. Swallow, Int. J. Radiat. Phys. Chem. 7 (1975) 363–370.
[31] C.H. Lee, H.B. Park, Y.M. Lee, R.D. Lee, Ind. Eng. Chem. Res. 44 (2005) 7617–7626.
[32] M. Aoki, H. Uchida, M. Watanabe, Electrochem. Commun. 7 (2005) 1434.
[33] V.O. Mittal, H.R. Kunz, J.M. Fenton, J. Electrochem. Soc. 153 (2006) A1755–A1759.
[34] T. Kinumoto, M. Inaba, Y. Nakayama, K. Ogata, R. Umebayashi, A. Tasaka, Y. Iriyama, T. Abe, Z. Ogumi, J. Power Sources 58 (2006) 1222–1228.
[35] D.E. Curtin, R.D. Lousenberg, T.J. Henry, P.C. Tangeman, M.E. Tisack, J. Power Sources 131 (2004) 41–48.

[36] S.A.M. Ali, P.J. Doherty, D.F. Williams, J. Appl. Polym. Sci. 51 (1994) 1389–1398.
[37] W.G. Barb, J.H. Baxendale, P. George, K.R. Hargrave, Trans. Faraday Soc. 47 (1951) 462–500.
[38] Y.K. Chong, G. Moad, E. Rizzardo, S.H. Thang, Macromolecules 40 (2007) 4446–4455.
[39] M. Danilczuk, A. Perkowski, S. Schlick, Macromolecules 43 (2010) 3352–3358.
[40] M. Danilczuk, F.D. Coms, S. Schlick, Fuel Cells 8 (2008) 436–452.
[41] L. Ghassemzadeh, M. Marrony, R. Barrera, K.D. Kreuer, J. Maier, K. Müller, J. Power Sources 186 (2009) 334–338.
[42] T. Ishimoto, R. Nagumo, T. Ogura, T. Ishihara, B. Kim, A. Miyamoto, M. Koyama, J. Electrochem. Soc. 157 (2010) 1305–1309.
[43] Y. Okamoto, Chem. Phys. Lett. 389 (2004) 64–67.
[44] A. Bosnjakovic, M.K. Kadirov, S. Schlick, Res. Chem. Intermed. 33 (2007) 677–687.
[45] W.Y. Hsu, T.D. Gierke, Macromolecules 15 (1982) 101–105.
[46] K. Hongsirikarn, X. Mo, J.G. Goodwin Jr., S. Creager, J. Power Sources 196 (2011) 3060–3072.